CH8800258

SIN - PR-87-08.

CRYOGENIC DETECTORS

A. ZEHNDER
Swiss Institute for Nuclear Research
CH-5234 Villigen, Switzerland

A contribution to the Festschrift in honor of V.L. Telegdi's 65th birthday. To be published by North-Holland Physics Publishing, edited by K. Winter.

Swiss Institute
for Nuclear Research

CH-5234 Villigen
Switzerland

November 5, 1987

CRYOGENIC DETECTORS

A. ZEHNDER
Swiss Institute for Nuclear Research
CH-5234 Villigen, Switzerland

Abstract

A review of the development of cryogenic detectors and their applications in astrophysics, dark matter search, and $\beta\beta$-decay with emphasis on superconducting tunneling junctions.

A contribution to the Festschrift in honor of V.L. Telegdi's 65th birthday. To be published by North-Holland Physics Publishing, edited by K. Winter.

1 Introduction

Progress in physics is often linked to new detectors. Improved energy, time and spacial resolution allows deeper insight in physical processes and may reveal new structures.

The development of cooled semiconductor silicon and germanium diodes in the sixties is a typical example: High resolution gamma ray studies in nuclear reactions and mesic atoms experiments were possible and gave new information in the field of nuclear and atomic physics and allowed tests of fundamental laws.

Presently the development of new large scale detector systems, used in very high energy physics experiments, is very active. In the low energy range, the introduction of charge coupled devices allows improved spacial and energy resolution.

In the keV-region, high resolution can only be achieved via the well established diffraction spectrometers with the well-known disadvantage of a small throughput. There exist no efficient detectors for non-ionizing radiation such as coherent nuclear scattering of weakly interacting particles. The development of high resolution solid state detectors in the keV-region with the possibility of nuclear recoil detection is therefore highly desired. Such detectors applied in astro and particle physics would thus allow one to obtain new information not achievable otherwise.

Particles absorbed or scattered in a detector will lead to an energy deposit. In a first step, this primary energy will be converted in a very short time into a non-equilibrium state that will then slowly relax to its equilibrium. In this non-equilibrium state, there will be a coexistence of various excited modes, mainly excess charge carriers and excess phonons.

An ideal detector measures all of these excess quantities. The energy resolution is determined by the statistical variations of the measured as well as the unmeasured excess quantities. A more detailed analysis has to be given for each type of detector individually.

Three types of cryogenic detectors exist:

- Calorimeters/Bolometers
  This type is sensitive to the produced excess phonons and measures the deposited energy by detecting the heat pulses. Excess charge carriers should be used to produce phonons.

- Tunneling junctions
  This type is sensitive to excess charge produced by the Cooper pair breakup. Excess phonons should be used to break up Cooper pairs.

- Superheated superconducting granules (SSG)
  A SSG-detector consists of granules, the metastability of which is disturbed by radiation. The Meissner effect then causes a change in the field distribution of the applied external field, which can be detected.

The present paper discusses the basic principle of calorimetric and tunneling junction detectors and some of their applications.

2 Bolometers

Principle

Bolometers are calorimeters of a small size. Simon[1] was the first to suggest the use of small low-temperature calorimeters. Niinikoski[2] pointed out in 1975 that single particles could be detected in this way. Experimental work was started in about 1983 by various groups [3,4,5]. An overview is given in Ref. 6 and references cited therein.

In principle the detector works as follows: after absorbing an energy E in a material with the specific heat C_v the temperature rise is

$$\Delta T = E/C. \tag{1}$$

In crystalline insulators at low temperature, the lattice vibrations (phonons) represent the dominant component of the specific heat C. The lattice specific heat decreases like T^3. Therefore to obtain large $\Delta T/T$ one is forced to work with small detectors (≤ 1 mm^3) and at low temperature (≤ 300 mK). The temperature rise is normally detected by the voltage drop across a thermistor in contact with the detector. Nevertheless, as discussed in chapter 3, there are alternative readout methods via superconducting tunneling junctions.

The equilibrium temperature is reached in a time $\tau = C/G$ in a few milliseconds via thermal links with the conductivity G.

The theoretical estimates of the resolution is treated by Moseley et al.[7] and summarized as follows:

In an ideal detector, the uncertainty of the measured energy depends on the quadrature sum of the magnitude of three noise signals caused by the temperature variations:

- thermal fluctuations ("phonon noise"),
- Johnson noise of the thermistor,
- Johnson noise due to the load resistor of the amplifier.

The contributions of the Johnson noise can be minimized by a careful detector design. Therefore the prevailing noise is caused by the thermal fluctuation. It can be estimated to be proportional to the square root of the number of phonon modes $\sqrt{CT/kT}$ times the energy per phonon mode kT, yielding

$$\Delta E_{rms} = \eta\sqrt{kT^2C} \tag{2}$$

where η contains all the information on thermistors and thermal links ($1.5 < \eta < 2$)[7]. The ideal energy fluctuation ΔE_{rms} for a $500 \times 500 \times 25$ μm^3 Si-crystal at a bath temperature of 100 mK ($C = 4 \cdot 10^{-15}$ J/K) should be $\Delta E_{rms} = 0.2$ eV. This resolution has not yet been obtained, but it shows the potential of this type of detector. The experimental limits are discussed below.

In a realistic thermal detector not all the energy of the radiation is transformed into heat in a short time. The NASA/Wisconsin group[3] estimates that only about 70% of the energy deposited in a silicon detector is promptly converted into phonons. The remaining 30% of the energy produces electron-hole pairs via ionization. They recombine only partly; some will be trapped by impurities and defect sites in the semiconductor crystal. As long as the electron is trapped on one of these sites, its energy is lost. The energy fluctuation due to those losses is

$$\Delta E_{def} = \sqrt{pE_o \Delta E_{gap}} \tag{3}$$

where p is the fraction of the initial energy E_o lost in charge trapping and ΔE_{gap} is the energy needed to populate a defect site. For $p \simeq 0.1$, $E_o \sim 6$ keV and $\Delta E_{gap} \sim 1/2$ eV one gets $\Delta E_{def} \approx 20$ eV, which is much larger than the ideal resolution. The NASA/Wisconsin Group solved this problem by absorbing the energy in a thin film of a semiconductor with a small band gap like HgCdTe attached to their silicon bolometer. It offers low heat capacity, therefore does not significantly contribute to the thermal noise fluctuation and it is relatively free of trapping sites.

Experiments

Experimental works were done by various groups, mostly detecting 5 MeV α-particles; so far only the NASA/Wisconsin group was able to observe the 6 keV Mn x-ray with an excellent energy resolution of about 17.4 eV FWHM[6], which is about a factor of 8 better than the best resolution achieved with LN_2 cooled Si-detectors (150 eV). The x-rays were absorbed in a 500 μm square 10 μ thick HgCdTe semiconductor. The experiments were performed at 80 mK. By sampling the baseline at random, a value of 13 eV FWHM was found for the thermal contribution to the overall system noise. This compares well with the expected 8 eV on the basis of the total system heat capacity. The 11 eV of excess broadening on the x-ray peaks may be due to non-uniform response across the detector or by residual thermalization noise.

3 Superconducting Tunneling Junctions

Principle

The basic understanding of this kind of detector was mainly worked out at the TH-Munich and at the Swiss Institute for Nuclear Research [8,9,10]. The possibility of using superconductors as detectors for ionizing radiation has been demonstrated for the first time in 1969 by Wood and White[11] and reviewed in various papers around 1981 by Kurakado and Mazaki[12]. In this type of detector the deposit energy is converted into excess quasiparticles (excited electronic states) resulting from the breakup of Cooper pairs. This charge is then collected via a tunnel barrier, similar to a semiconductor diode detector. The potentially high energy resolution arises from the fact that the quasiparticles are separated from the Cooper pairs by a gap Δ of the order of 1 meV, which is about 1000 times smaller than the gap of a Si/Ge-semiconductor detector.

Assuming Poisson statistics the energy resolution is given by

$$\Delta E_{rms} = \sqrt{f \cdot E_o \epsilon} \tag{4}$$

where $\epsilon \geq \Delta$ is the minimal ionizing energy of the detector. This relation clearly favors small energy gaps. The Fanofactor f≤1 describes the anti-correlation of the produced charge.

As an example, a semiconductor Si-diode with f=0.31 and $\epsilon = 3.61$ eV yields

$$\frac{\Delta E_{FWHM}}{E}(@\,6\,keV) \sim 3\% \tag{5}$$

whereas a superconducting Sn-detector with $f \simeq 1$ and $\Delta = 0.585$ meV should yield

$$\frac{\Delta E_{FWHM}}{E}(@\,6\,keV) \approx 0.1\%. \tag{6}$$

In contrast to semiconductor detectors, in superconducting detectors the energy deposited in phonons is not a priori lost. This is due to the fact that the maximum phonon energy of 10 - 20 meV is larger than the gap of a superconductor, but much smaller than the band gap of a semiconductor. In fact, phonons play an essential role in the understanding of superconducting tunneling junctions.

The following gives a short introduction to the physics of such devices. Further information can be found in the papers of Chang and Scalapino[13)] and Kaplan et al.[14)].

The superconducting tunneling junction detector consists of two metallic films (at least one being superconducting) separated by a thin insulating barrier, which allows quantum mechanical tunneling of the quasiparticles. An excess number of those particles leads to an excess tunneling current that can be integrated. Such devices were first used by Giaever[15)] to study the physics of quasiparticles.

If the junction is biased above a potential $V \geq (\Delta_1 + \Delta_2)/e$ (where Δ_1, Δ_2 are the gaps of film 1 and 2 respectively), it displays ohmic behavior $\delta V = R_N \cdot \delta I$. Assuming that the tunnel matrix element is independent of the energy, for R_N one gets

$$R_N = \frac{\tau_{tun}}{e^2 N_o V} \tag{7}$$

where τ_{tun} is the tunneling time, e the electronic charge, N_o the single spin density at the Fermi energy ($\sim 1.4\ 10^{22}$/eV/cm^3 for Sn) and V is the volume of the junction. R_N is an important quantity, because it allows an easy calculation of the tunnel rate τ_{tun}^{-1}, which typically is about 10^6 sec^{-1}.

Incident radiation will mostly produce a photoelectron that, in a very short time ($\sim 10^{-11}$ sec), will relax[14)] to the band gap while emitting phonons. Once the quasiparticles reach the minimal energy Δ, they can recombine to a Cooper pair emitting a 2Δ phonon. This 2Δ phonon together with the initially produced phonons of the energy $E \geq 2\Delta$ are very likely absorbed, owing to the short phonon pair breaking time $\approx 10^{-10}$ sec (phonon trapping). Detailed analysis leads to the so-called Rothwarf-Taylor equations[16)]: A set of coupled differential equations for phonons and quasiparticles in both films. Details are found in the thesis of Twerenbold[8)]. At sufficiently low temperature (T/T_c), the phonons disappear in a short time ($\sim$ 5 nsec) leaving quasiparticles, which either tunnel, recombine, or diffuse out of the junction. The number of tunneling quasiparticles can be estimated

$$N_{tunn} = N_o \frac{\tau_{tunn}^{-1}}{\tau_{tunn}^{-1} + \tau_{rec}^{-1} + \tau_{diff}^{-1} + \tau_{loss}^{-1}} \tag{8}$$

where $N_o = E_o/\Delta$ is the total of initial quasiparticles, τ_{tunn}^{-1} is given by Eq.7, and the recombination rate [14] is

$$\tau_{rec}^{-1} \simeq (\pi)^{1/2}(2\Delta/kT)^{5/2}(T/T_c)^{1/2} exp(-\Delta/kT) \cdot \tau_o^{-1} \quad (9)$$

τ_o is 2.30 nsec for Sn, other values can be found in Ref. 14. The recombination time τ_{rec} is about 100 μsec at $T/T_c \approx 0.1$; this means that it is much longer than τ_{tun}. However, owing to its strong temperature dependence, $\tau_{rec} \approx \tau_{tun} \approx 1\mu sec$ at $T/T_c \approx 0.2$.

The diffusion time τ_{diff} was experimentally studied [17], and was shown to depend on the special geometry of the junction. Additional losses due to various processes are included in an effective loss time τ_{loss}.

Experimental Work

The best resolution so far was obtained by the SIN group with Sn/SnO/Sn junctions which had surfaces of about 50 × 50 μm^2. These junctions are made by photolithographic stencil lift-off technique. The current leads are about 5 μm wide, thus diffusion out of the junction area is suppressed. The tunnelled charge is collected via a charge sensitive amplifier; at low temperature (0.4 K) a total of about 3 × 10^6e are integrated. This gives an effective gap Δ_{eff} of about 2 meV, which has to be compared with the intrinsic gap of 0.6 meV. Fig. 1 shows the temperature dependence of the signal compared with the prediction of the above discussed model. The decrease of signal amplitude with increasing temperature is mostly due to the enhanced recombination of quasiparticles at a higher temperature.

Fig. 2 displays a typical energy spectrum of Mn x-rays, the dotted line indicating the best resolution of Si(Li) detectors. One sees a marked improvement. Nevertheless, the resolution of about 47 eV FWHM is not as good as the expected 5 eV. The baseline noise (mostly 1/f noise of the junction device) amounts to 24 eV FWHM as measured with a pulser. Correcting the measured resolution for the baseline noise, one obtains an intrinsic junction resolution of 40 eV.

Detailed measurements of the diffusion property[17] of quasiparticles showed that an additional loss mechanism has to be included in our model. Its loss time is about 10-30 μsec and therefore is important at low temperatures, along with the tunneling time, in determining the effective life time of quasiparticles. It could be attributed to the quasiparticle trapping and later recombination in sub gap structures of individual grains (crystals). Further work is needed to clarify this point.

Fig. 3 shows an energy vs time plot: One observes a repetition of the K_α, K_β line, due to absorption of the x-rays in the upper and the lower film respectively. As explained in detail in Ref. 8, this process can be understood in the following way (see Fig. 4): the incoming radiation breaks up Cooper pairs and generates quasiparticles. As appears in Fig. 4, a quasiparticle of the film with the higher potential (film 1) can tunnel. Quasiparticles of the film with the lower potential (film 2) can recombine with an electron of a Cooper pair, forming a Cooper pair in film 2 and, by energy conservation, generating a quasiparticle in film 1. In both cases a current of equal sign is produced. In addition, one can see that, in a single step, a symmetric situation (a quasiparticle on each side) is formed. If there are no loss mechanisms, the above described processes could be repeated, leading to a current amplification.

An interesting extension of superconducting tunneling junctions was proposed by Booth[19]. His idea consists of trapping quasiparticles in a two stage process, as shown in Fig. 5 (from Ref.19). Radiation is absorbed in a superconductor with a gap Δ_1 and generates quasiparticles. They diffuse fast and will be de-excitated by phonon emission in an adjacent superconductor with a gap Δ_2.

If the difference between the gaps Δ_1 and Δ_2 is larger than $2\Delta_2$, the phonons emitted during de-excitation can break up Cooper pairs in superconductor 2, resulting in the multiplication of quasiparticles. In addition, the tunnel rate of the trapped quasiparticles is strongly enhanced, owing to their smaller diffusion volume (see Eq.7). This leads to a fast rise time, which is needed for timing applications. At SIN a Pb alloy/Sn/SnO/Sn junction was fabricated that showed a marked increase in the rise time as seen in Fig. 6. The thickness was about 0.5 μm for Pb and about 0.1 μm for each Sn layer. The rise time increased to about 1 μsec compared to about 20 μsec in an Sn/SnO/Sn junction.

In conclusion, SIS-tunneling junctions have interesting properties, which are fairly well understood. Possible applications are discussed below.

4 Application

High Resolution X-ray Spectroscopy

With the scheduled launch of large x-ray observatory satellites in the USA (AXAF) and in Europe (XMM), there exists a need for detectors with a high throughput and a high resolution in the 0.1-10 keV range. This region is rich in (highly excited) x-ray lines of cosmically abundant elements. Grating instruments have the required resolution, but are too inefficient, whereas solid state detectors have too poor a resolution to resolve the different ionization states. A 5×5 mm^2 cryogenic detector with about 10 - 15 eV resolution would be an ideal instrument for this interesting spectroscopic problem.

As shown above, bolometric detectors have reached the required resolution. However, the operation temperature of less then 100 mK and the slow ($\sim$1 msec) pulses are disadvantages for some applications.

SIS tunneling junctions have not yet reached the required resolution, but no limiting factor has been found. They are rather fast ($\sim$ μsec) and can operate at $T/T_c \approx 0.15$ which for Pb is about 0.5-1 K. Therefore, junctions pose a less stringent problem for the supporting space cryogenics than do bolometers. However, their small size requires large arrays.

β-Decay in true Calorimeters

Experiments that require accurate measurements of energy differences between an initial and a final state are often hampered by not accurately knowing the energy losses in the source and in the detectors as well as effects of the initial and the final state interactions. A true calorimeter that measures the Q-value with a time constant which is long compared with the life time of the decay process could solve this problem. A typical example is the measurement of the end point of the tritium β-decay spectrum to place a limit on the neutrino mass. Tritium could be implanted in a detector (SIS-junction or bolometer-absorber) and would not be subject to the shortcomings of a separated source-detector system. The resolution is comparable with the overall resolution that present experiments obtained.

Since all the β-decays are measured, the count rate limitations are quite severe, but a calculation indicates that it would be practical to establish a mass limit of about 10 eV for the ν_e that would be relatively free of systematic errors [19].

The study of the shape of β-decay spectra of polarized or aligned nuclei gives information on induced terms (weak magnetism, second class current). Cryogenic detectors offer in principle the possibility of calorimetric high resolution measurements of these spectra.

Neutrino and dark Matter Detection

Dark galactic halos may be needed to solve the problem of the "missing mass" in order to close the universe. This missing mass could make up to 90% of the total [20].

Many particles were suggested for non barionic dark matter candidates; if these particles are weakly interacting with nuclei, there may be a possibility of observing them with advanced cryogenic detectors. Coherent neutrino scattering off nuclei has so far never been observed in laboratories, but it plays an important role in supernova dynamics [21]. The detection of these weakly interacting particles (WIP's) should be possible by observing the recoil of elastic scattering of WIP's off nuclei in a large insulating crystal[22,23].

The recoil produces (after fast cooling to about 10-20 K) quasi-free phonons (ballistic phonons) that at a sufficiently low temperature travel through the crystal with no dispersion and no scattering. Nevertheless, a strong focusing effect occurs within the crystal. This well studied effect has its origin in the anisotropy of the medium, and leads to different phase velocities in different directions[24]. Detailed calculations were done in Ref. 22. Fig. 7 shows the distribution of ballistic phonons on a Si-crystal surface. The readout of these phonons could be achieved through thermistors or, because of the high pair breaking rate of $\geq 2\Delta$-phonons, through tunneling junctions.

The recoil energy and rate for particles with coherent weak coupling to the target nucleus can be estimated as follows:[25] If a nonrelativistic halo particle with mass m and velocity v scatters off a target nucleus M, the recoil energy is $T_{max} = (2mv)^2/2M$ at the most. For v = 200 km/sec (virial velocity) and for a threshold energy of 10 eV per phonon for a readout detector with an overall efficiency of 2% per strip, one should be able to set a limit for a WIP's of $p \geq 2.6$ MeV/c, corresponding to a mass of halo particles of about 3.9 GeV/c^2.

The rate can be calculated in the standard model for massive WIP's with vector coupling to Z_o-bosons.

$$R = 4.2 events/kg\, day[\frac{\sigma/A}{10^{-38}cm^2}] \cdot [\frac{\rho}{0.4GeV/cm^3}] \cdot [\frac{v}{200km/sec}] \qquad (10)$$

where ρ is the mass density of the halo particle. ρ is estimated to be $\rho = 0.4$GeV/cm^3.

The reduced cross section σ/A is given by:

$$\sigma/A = (2.10^{-39}cm^2)[\frac{4mM}{(m+M)^2}]Y(N-(1-4sin^2\theta)Z)^2 \tag{11}$$

where N and Z are the numbers of neutrons and protons respectively, and Y is the weak hyper charge.

The event rate for coherent scattering of WIP's off Si-nuclei is given in Table 1. The model-dependent hyper charge Y is assumed to be 1.

Mass (GeV/c^2)	Recoil (keV)	Rate (spin-independent) /kg/day	Rate (spin-dependent) /kg/day
1	0.03	23	4
5	0.82	86	15
10	3.3	130	22
100	330	110	19

Table 1: Recoil energy and rates for coherent scattering off nuclei of WIP's

It is possible that dark matter consists of particles that interact with nuclei only via spin-dependent forces. In Table 1, we list as an example the rates of interactions between massive photinos and nuclei via the exchange of massive scalar quarks. The values in Table 1 were calculated assuming that $M_{\tilde{Q}} \simeq 100$ GeV and that the spin-dependent nuclear matrix elements are of order unity. Details are given in Ref. 25.

The cross section for vector neutral-current scattering of neutrinos off nuclei is given by

$$\sigma_{tot} = G_F^2 E^2 (N - Z(1 - 4\,sin^2\theta_w)^2/4\pi \tag{12}$$

and, in contrast to the ν-e scattering, it is independent of the neutrino type. The event rate for ^{8}B-solar neutrinos was calculated in Ref. 23, yielding a small recoil energy and a rate of 0.16 events /ton/day. This is most probably too small to be detected amidst the background.

Nuclear reactors are a powerful source of antineutrinos. For a detector located at a distance of 10 m from the reactor core with a flux of $2 \cdot 10^{13}/cm^2$/sec, one would get events with a recoil energy in the range of 0.5 keV<T<6 keV at a rate of ~40 kg/day. An interesting possibility arises by simultaneously detecting the recoil electrons from ν-e scattering in the same detector. They deposit a much greater energy (up to ≤10 MeV) at a rate of 4 events/kg/day. In contrast to the coherent ν-N scattering, the electron scattering is sensitive to ν-oscillation; a movable recoil detector would therefore be an interesting tool to study ν-oscillation.

Finally, neutrinos from a supernova would produce about 1 event/ton in the pulse that lasts a few seconds. A detector of several tons would be needed. Its construction is not possible with techniques of today.

In conclusion, a cryogenic ballistic phonon detector of a few kg may be a promising instrument to study the existence of certain dark matter candidates and the properties of reactor neutrinos. However, more studies must be made, particularly with regard to the background and to the detection of the ballistic phonons.

First results are promising, proving that basic ideas are correct. Therefore a major effort is justified.

$\beta\beta$-Decays

It was pointed out by Ref. 26 that today's underground detectors sets limits to $\beta\beta$-decays that are hard to improve. The neutrinoless $\beta\beta$-decay experiments are of particular interest to the testing of the lepton number non-conservation. The transition (A,Z)→(A,Z+2)+2e would manifest itself in a monoenergetic line at the appropriate energy; the best detection efficiency is clearly given if the detector is identical with the source. Cryogenic detectors should in addition yield a better energy resolution than semiconductor detectors. It is also advantageous to have a larger selection of target materials. So far $\beta\beta$-decay search was restricted to Ge(Li)-detectors and to Se and Xe TPC chambers.

Calorimetric detectors must operate in a temperature range, where the material possesses a low specific heat (Eq. 1).

- In crystal insulators the specific heat is given by the dominant lattice specific heat. In this kind of detector thermalization of phonons is only achieved by scattering off crystal faults and off surfaces. The resolution may also be nonoptimal, owing to charge carrier trapping, as demonstrated by Ref.3 in pure Si.
- Normal conducting metals are not well suited, because the specific heat is large and determined by conduction electrons $C_e \propto T$.
- Superconductors at low temperature have low specific heat, but the energy is not stored in phonons, but in excess quasiparticles as explained above. If the surface is covered with tunneling junctions, a readout is in principle possible. The tunnel rate is extremely slow, owing to the large volume (see Eq.7). An interesting possibility arises by coating the surface of the superconductor with tunneling junctions of a smaller gap, thus using the effect of trapping quasiparticles on the surface, as described above. The tunnel rate is enhanced (see Fig. 6).

As an example, we consider the ^{100}Mo $\beta\beta$-decay. ^{100}Mo, having a $\beta\beta$-decay transition energy of 3033 keV is a superconductor with a high T_c in a binary compound. The sensitivity is estimated in Ref. 26 to be $5{\cdot}10^{24}$ years for a 450 kg Mo cube. This limit is well below the present limits for the $\beta\beta$-decay lifetime; further studies are therefore justified.

Conclusion

The potential of cryogenic detectors has been demonstrated in experimental work. A few examples show possible applications. However, further studies are needed and should be pursued in various laboratories.

References

1) S. Simon, Nature 135, 763 (1935)

2) T.O. Niinikoski, in "Liquid and Solid Helium" (Halsted, New York, 1975) p. 145

3) D. McCammon et al., J. Appl. Phys. 56, 1263 (1984)

4) N. Coron et al., Nature 314, 75 (1985)

5) C. Borango et al., Cryogenics 24, 681 (1984)

6) D. McCammon et al., in Proc. 18th Conference on Low Temp. Phys., Kyoto, (1987). Jap. J. Appl.Phys., 26 Supp. 26.

7) S.H. Moseley, J.C. Mather and D. McCammon, J. Appl. Phys. 56, 1257 (1984)

8) D. Twerenbold, Phys. Rev. B34, 7748 (1986)

9) D. Twerenbold and A. Zehnder, J. Appl. Phys. 61, 1 (1987)

10) H. Kraus et al., Europhys. Lett. 1, 161 (1986)

11) G.H. Wood and B.L. White, Appl. Phys. Lett. 15, 237 (1969)
G.H. Wood and B.L. White, Can. Journ. Phys. 51, 2031 (1973)

12) M. Kurakado and H. Mazaki, Phys. Rev. B22, 168 (1980)
M. Kurakado and H. Mazaki, Nucl. Instr. and Meth. 185, 141 (1981)
M. Kurakado and H. Mazaki, Nucl. Instr. and Meth. 185, 149 (1981)
M. Kurakado, Nucl. Instr. and Meth. 196, 275 (1982)
M. Kurakado, J. Appl. Phys. 55, 3185 (1984)

13) J.J. Chang and D.J. Scalapino, Phys. Rev. B15, 2651 (1977)

14) S.B. Kaplan et al., Phys. Rev. B14, 4854 (1976)

15) I. Giaever, Phys. Rev. Lett. 5, 147 (1960)
I. Giaever, Phys. Rev. Lett. 5, 464 (1960)
I. Giaever and K. Megerle, Phys. Rev. 122, 1101 (1961)

16) A. Rothwarf and B.N. Taylor, Phys. Rev. Lett. 29, 27 (1967)

17) W. Rothmund and A. Zehnder to be published

18) N.E. Booth, Appl. Phys. Lett. 50,2 (1987)

19) D. McCammon et al., Neutrino Mass and Low Energy Weak Interactions. Telemark 1984, eds. V. Barger and D. Cline (World Scientific Singapore 1985) p. 329

20) G.R. Blumenthal et al., Nature 311, 517 (1984)

21) E. Commins and P. Bucksbaum, Weak Interactions of Leptons and Quarks (Cambridge Univ. Press, New York, 1983) and references therein

22) B. Cabrera, J. Martoff and B. Neuhauser, Nucl. Instr. and Meth. (submitted), Standford Preprint BC44-86 (1986)

23) B. Cabrera, L.M. Krauss and F. Wilczek, Phys. Rev. Lett. 55, 25 (1985)

24) G.A. Northrop and J.P. Wolfe, Phys. Rev. B24, 6196 (1980)

25) M.W. Goodmann and E. Witten, Phys. Rev. D31, 3059 (1985)

26) E. Fiorini and T.O. Niinikoski, Nucl. Instr. and Meth. in Phys. Research 224, 83 (1984)

Figure captions

Figure 1 Temperature dependence of the rise time and fraction of the initially produced charge (10^7e). The parameters are taken from Ref.8 and 17.

Figure 2 Energy spectra from Mn x-rays measured with a Sn/SnO/Sn tunneling junction. The dotted line corresponds to the best resolution obtained with LN_2 cooled Si-detectors.

Figure 3 2-dimensional spectra from Sn-junctions on fused silica substrate. The K_α, K_β lines resulting of Mn x-ray absorption in the lower and upper film are clearly resolved.

Figure 4 Tunneling processes in a junction with both films superconducting. For details see text.

Figure 5 Energy diagram showing trapping of excess quasiparticles produced in superconductor S_1 by an adjacent superconductor S_2 of lower gap.

Figure 6 Rise time of single pulses from a Mn x-ray source. The slow pulse corresponds to a tunneling time of about 4 μsec in a Sn/SnO/Sn tunneling junction. The fast pulse was produced by quasiparticle trapping as explained in the text.

Figure 7 Phonon focusing effect on a cubic crystal. The figure on the right side hints possible superconducting tunneling junction phonon readout strips. (From Ref. 22)

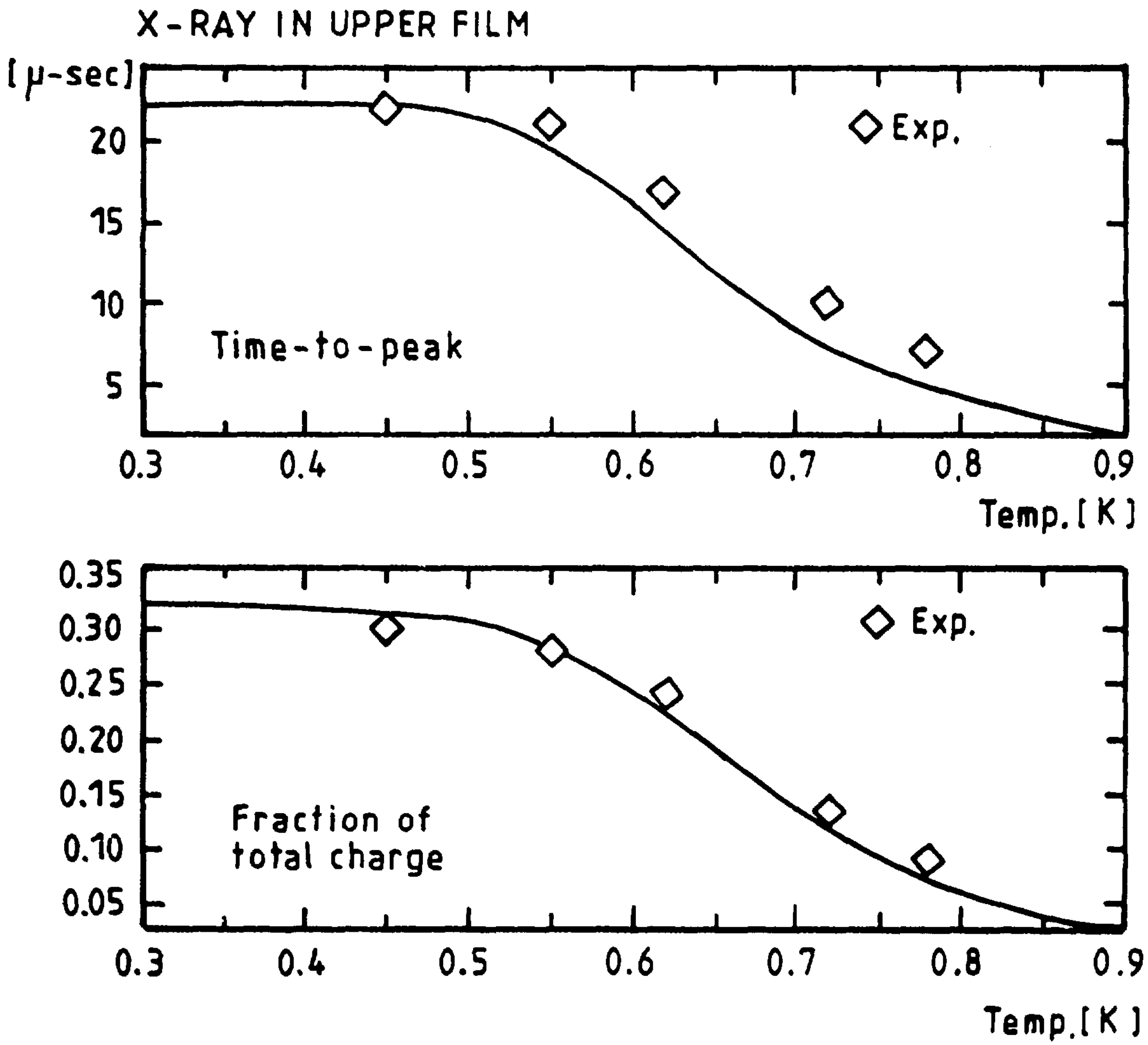
X-RAY IN UPPER FILM
[μ-sec]
20
15
10
5
Time-to-peak
Exp.
0.3
0.4
0.5
0.6
0.7
0.8
0.9
Temp.[K]
0.35
0.30
0.25
0.20
0.15
0.10
0.05
Fraction of
total charge
Exp.
0.3
0.4
0.5
0.6
0.7
0.8
0.9
Temp.[K]

Figure 1

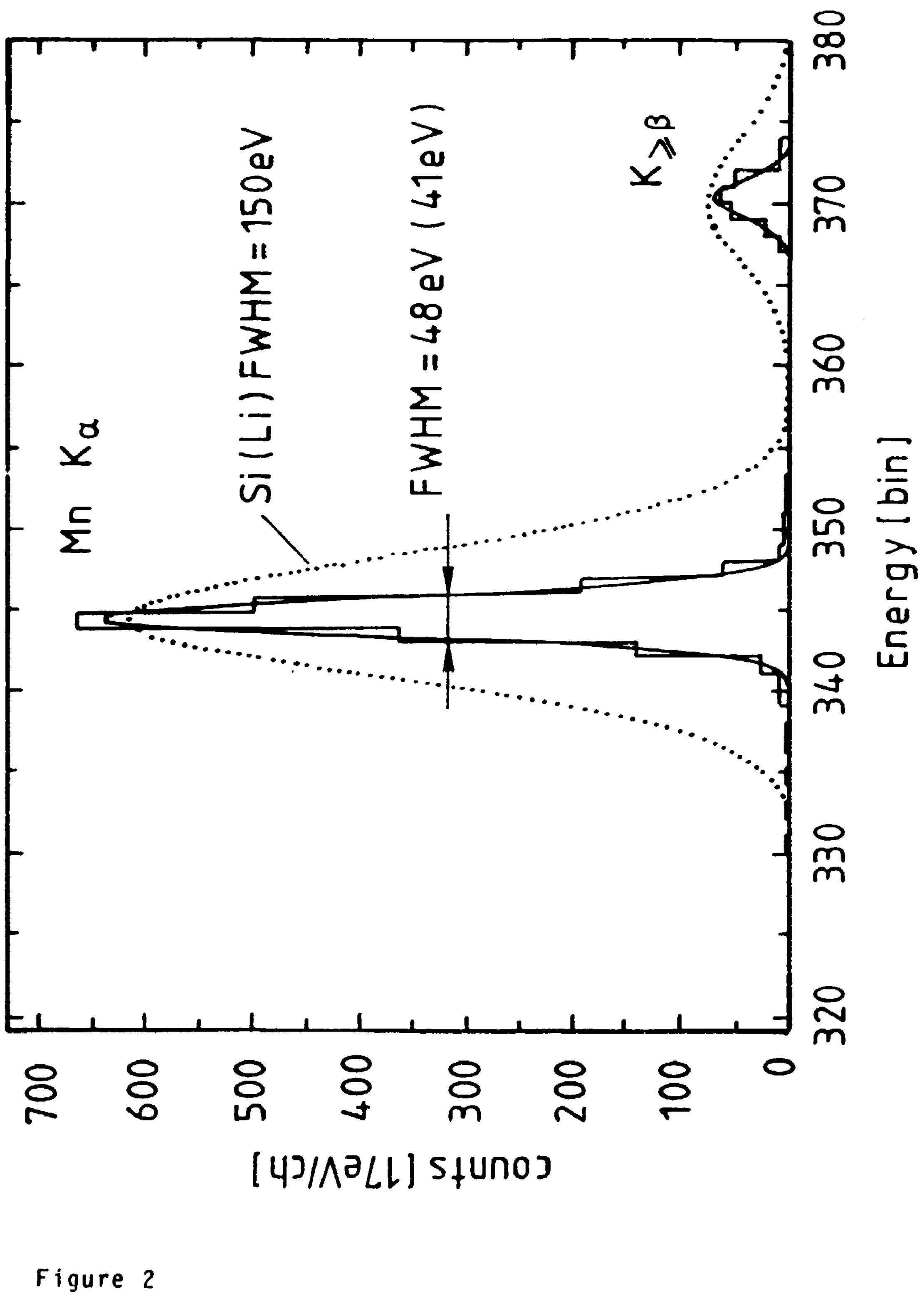
Mn Kα
Si (Li) FWHM = 150eV
FWHM = 48 eV (41eV)
K≥β
Energy [bin]
counts [17eV/ch]
320
330
340
350
360
370
380
0
100
200
300
400
500
600
700

Figure 2

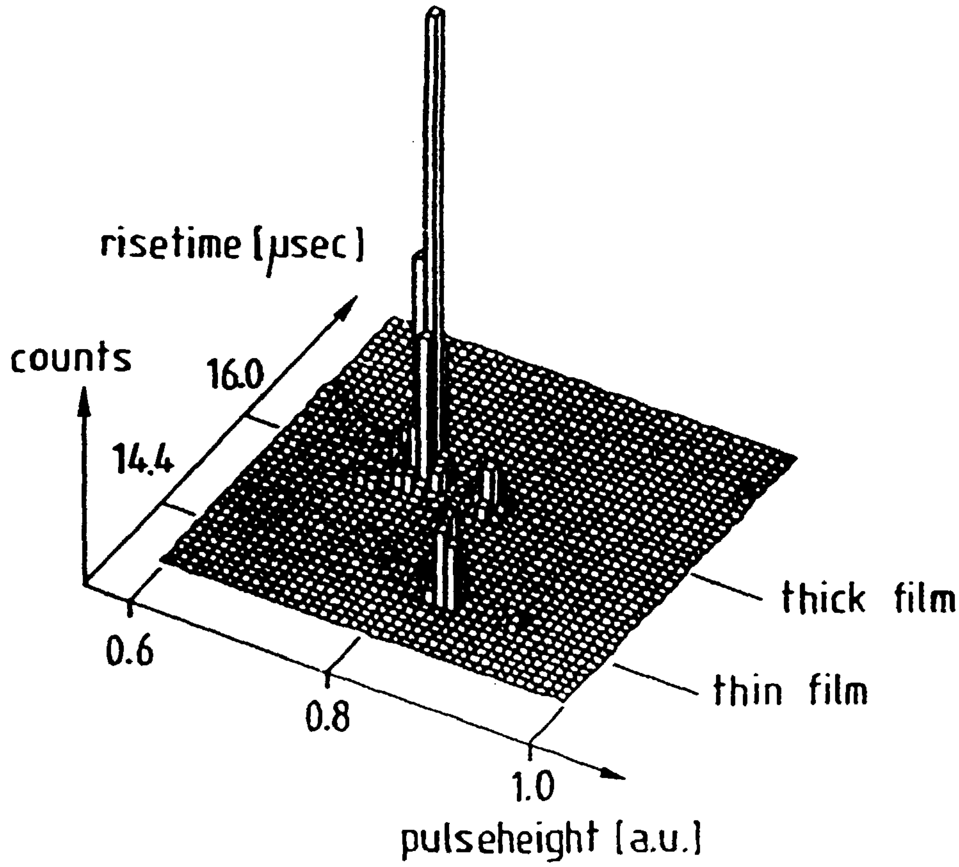
risetime [μsec]
counts
16.0
14.4
0.6
0.8
1.0
pulseheight [a.u.]
thick film
thin film

Figure 3

Figure 4

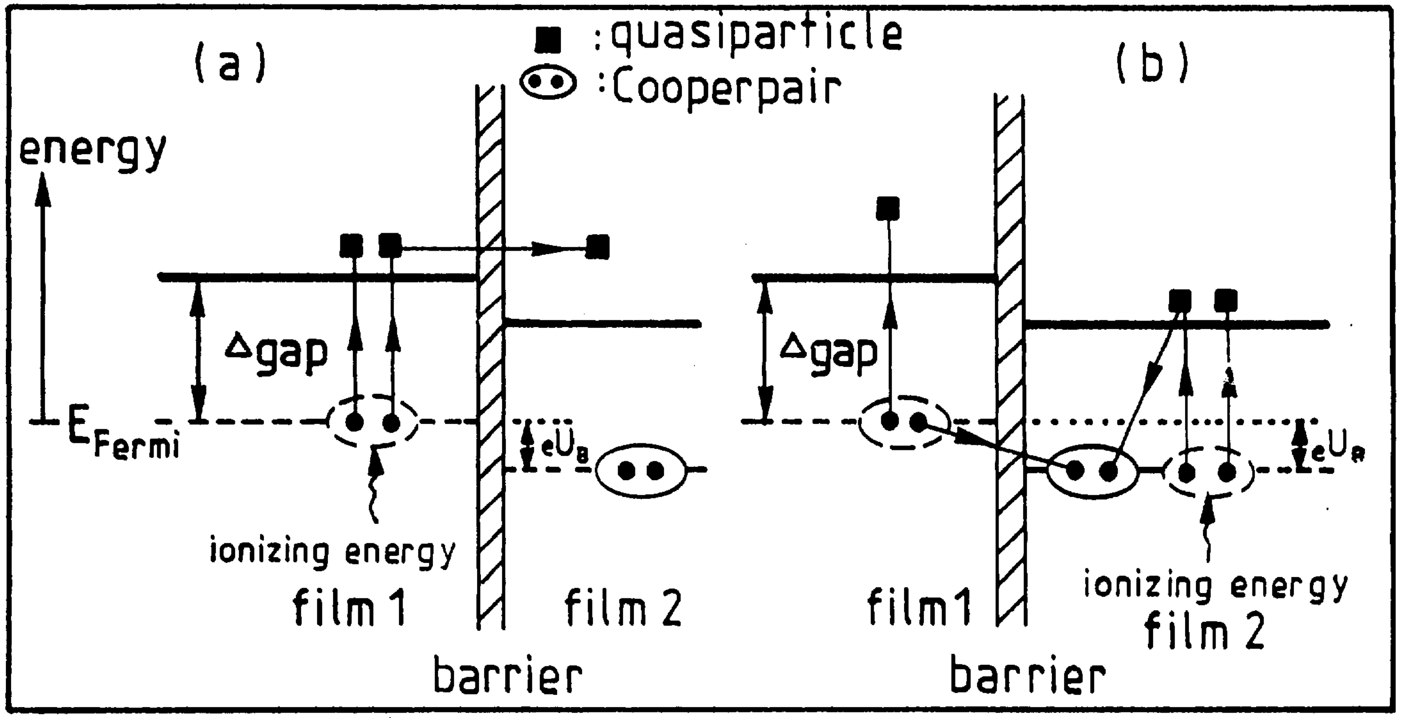

:quasiparticle
:Cooperpair
(a)
(b)
energy
Δgap
E Fermi
eU B
ionizing energy
film 1
film 2
barrier

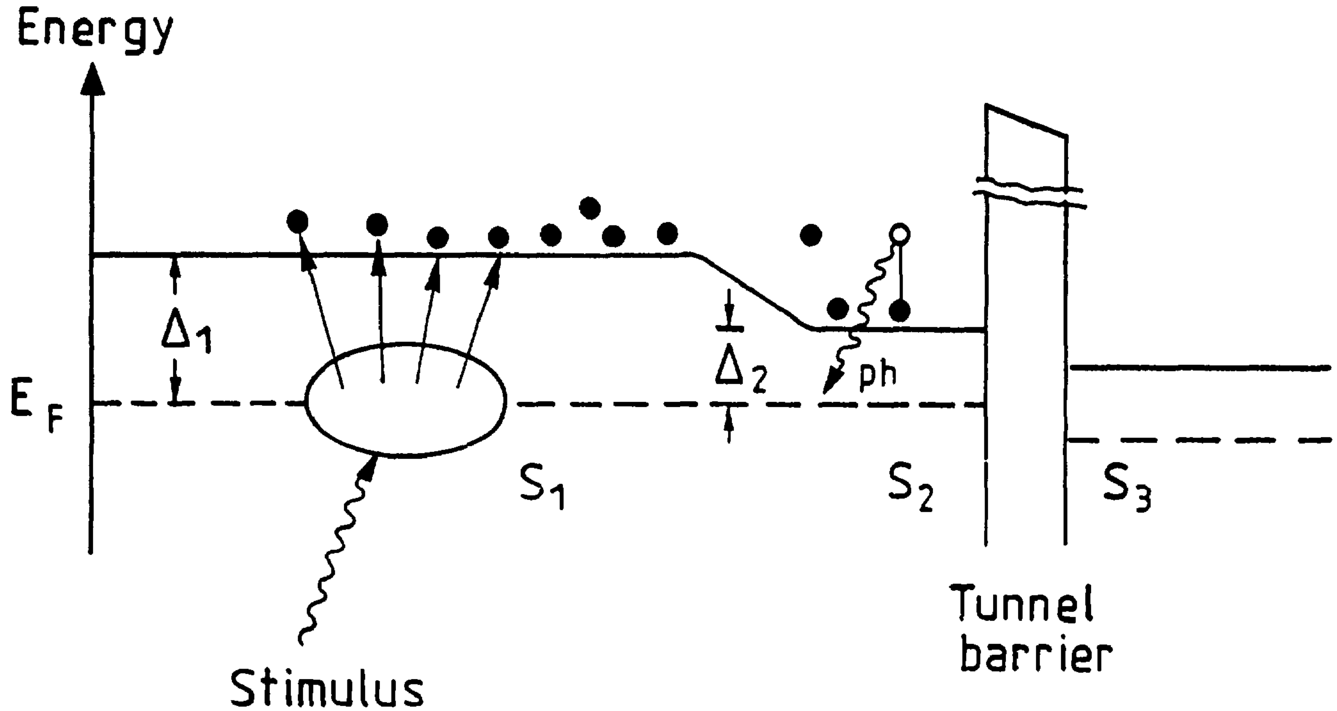

Figure 5

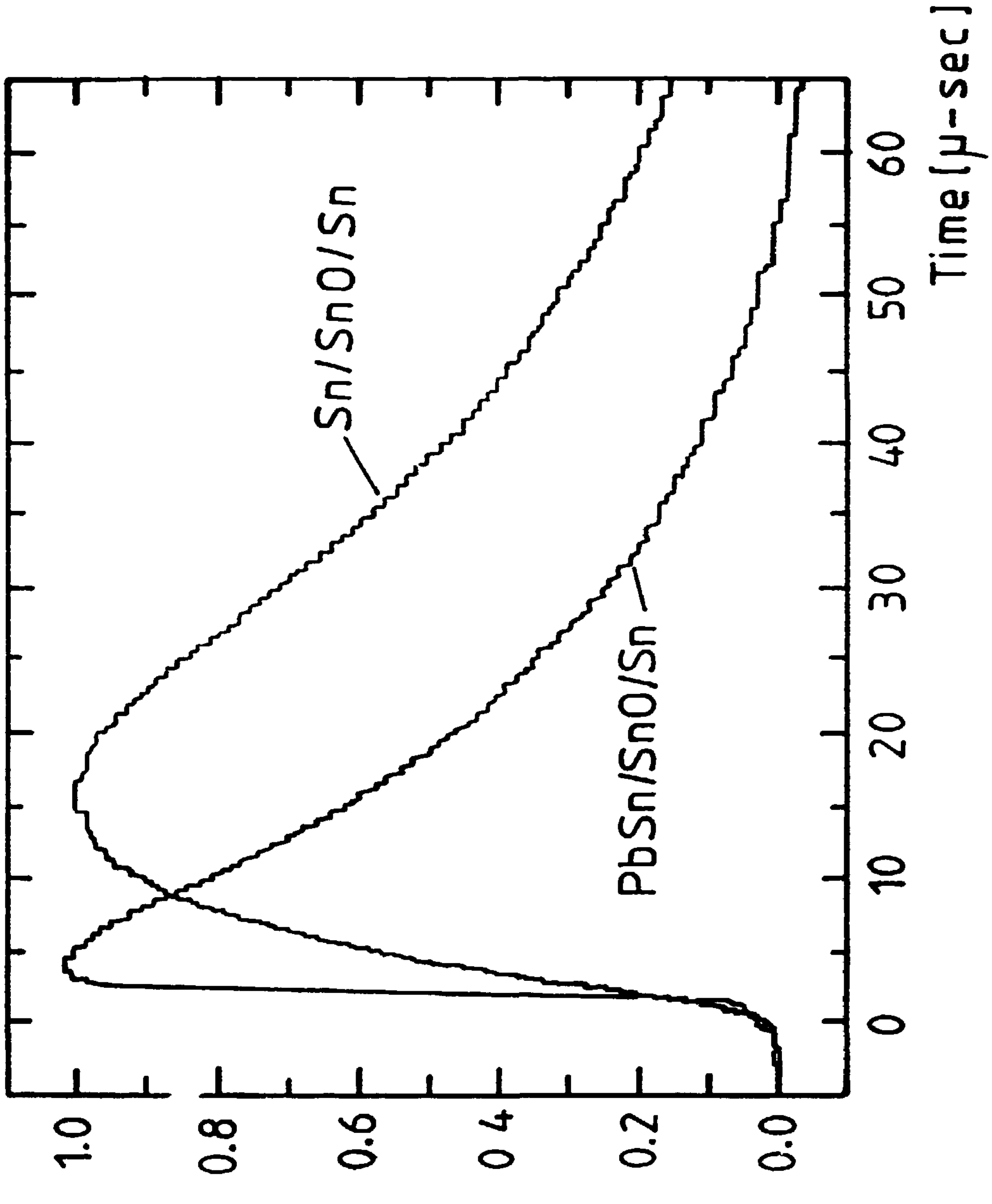

Figure 6

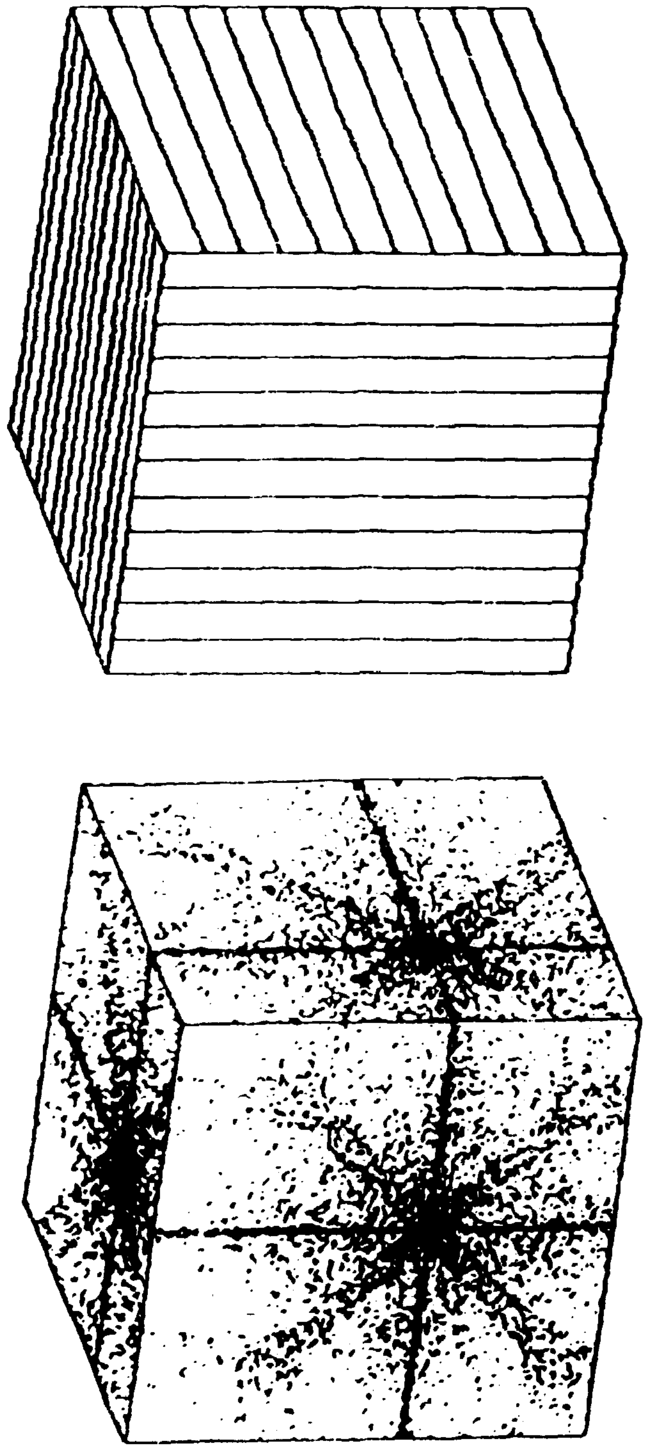

Figure 7